

Time Resolved ESR Study on the Photochemical Reactions of Pyrene and Nitroxide Radical System in Micelle; Formation of Spin-Correlated Pyrene Cation–Nitroxide Pairs

Akio Kawai,* Atsushi Shikama, Masaaki Mitsui, and Kinichi Obi#

Department of Chemistry, Graduate School of Science and Engineering, Tokyo Institute of Technology, 2-12-1 Ohokayama, Meguro-ku, Tokyo 152-8551

(Received November 13, 2000)

Time-resolved ESR (TR-ESR) spectra were measured in the laser excitation of aromatic compounds such as xanthone, bromopyrene, fluoranthene (Flt) and pyrene (Py) in sodium dodecyl sulfate (SDS) aqueous micellar system in the presence of 2,2,6,6-tetramethyl-1-piperidinyloxy (TEMPO). Net emission (Em) signals of triplet hyperfine (hf) lines of TEMPO were observed in xanthone– and bromopyrene–TEMPO systems. The chemically induced dynamic electron polarization (CIDEP) was explained by radical-triplet pair mechanism. Antiphase signals of TEMPO with Em in low-field side and enhanced absorption in high-field side (EA) of each triplet hf line were superimposed on net Em signals in Flt– and Py–TEMPO systems. The square laser power dependence of the EA signal suggests that the two-photon ionization of Flt and Py is related to the EA antiphase signal. Rate constants of the reactions occurring in SDS solution were determined by analysis of transient absorption decays in the Py–TEMPO system. The reaction rates of Py^+–TEMPO and $^3Py^*$–TEMPO in SDS solution were determined as $1.2 \times 10^6\ s^{-1}$ and $3.0 \times 10^5\ s^{-1}$, respectively, at the TEMPO concentration of 2 mM (M = mol dm^{-3}). According to these measurements, it was concluded that the EA CIDEP is due to spin-correlated radical pair (SCRP) of TEMPO and Py^+ which was formed in the electron transfer reaction from TEMPO to Py^+. Simulation of TR-ESR spectra was carried out using SCRP theory. From kinetic analysis of intermediates together with the simulation of TR-ESR spectra, it was concluded that both SCRP of Py^+–TEMPO and RTPM of $^3Py^*$–TEMPO contribute to the CIDEP of TEMPO.

Interaction between a radical and an excited state molecule during the excited state quenching process creates a non-Boltzmann distribution in electron spin levels of the free radical.[1,2] This non-equilibrium distribution in electron spin levels results in strong electron spin polarization, called chemically induced dynamic electron polarization (CIDEP),[3] which is usually detected by a time-resolved ESR (TR-ESR) method. We have been investigating the mechanism to create CIDEP in the radical-inducing quenching process of various excited molecules.[4] Chemically stable free radicals such as galvinoxyl and nitroxides were used in these studies. CIDEP generation in these systems has been understood in terms of the radical-triplet pair mechanism (RTPM), in which time evolution of a spin wavefunction of radical-triplet collision pair in the presence of the electron-electron dipolar interaction provides net polarization on a free radical.[1,2]

CIDEP intensity due to RTPM is usually stronger when the quenching occurs in micelle than in ordinary solutions.[5] The very low mobility of molecules in the micelle interior prolongs the lifetime of the radical-triplet collision pair; hence, the time evolution of spin wavefunction during the collision process results in large electron polarization on a free radical. This strong CIDEP should improve the signal-to-noise ratio in TR-ESR measurements and we anticipated that probing of CIDEP of free radicals would enable us to study the quenching process of excited states by free radicals in micelle. However, we realized that the probing of CIDEP was not a simple method of extracting the memory of quenching events in micelle. In some systems of 2,2,6,6-tetramethyl-1-piperidinyloxy (TEMPO) and excited molecules, we found that the chemistry of TEMPO with cation and electron produced by photoionization process gave undesirable CIDEP on TEMPO. This CIDEP is dominated by an antiphase structure (APS) of each hyperfine line. Spin-correlated radical pairs (SCRP) are one of the most important intermediates appearing in photochemical reactions and it is well known that SCRP spectrum is characterized by APS.[6–9] Appearance of CIDEP with APS in TEMPO-excited molecule systems suggests the existence of spin-correlated species and a strong APS signal unfortunately prevents us from taking a pure CIDEP spectrum of free radical due to an excited state quenching process in micelle. Therefore, it is definitely important to understand the photochemistry in these systems when we measure CIDEP as a probe of the excited state quenching process.

In this report, we analyze CIDEP patterns of TEMPO obtained in sodium dodecyl sulfate (SDS) micelle in much detail. Moreover, we measured transient absorption spectra and decays of intermediates produced in these systems. Initial photochemical process of TEMPO and excited molecule systems in SDS micelle interior will be described according to the results.

Present address: Department of Chemical and Biological Sciences, Japan Women's University, 2-8-1 Mejirodai, Bunkyo-ku, Tokyo 112-8681, Japan.

Experimental

TR-ESR Measurement. TR-ESR detection system consists of an X-band ESR spectrometer (Varian E-112) and a boxcar integrator (Stanford SR-250) to extract transient ESR signals synchronized with laser pulses.[10] The excitation light source was a XeCl excimer laser (Lambda Physik LPX 100, 20 ns duration time, 100 mJ/pulse). The laser power was attenuated to about 10 mJ at the cell in the microwave cavity for CIDEP measurements. The signals were collected at the repetition rate of 10 Hz. The microwave power was usually 15 mW.

Transient Absorption Measurement. A transient absorption detection system has already been described elsewhere.[11] An excitation light source was the XeCl excimer laser used in the TR-ESR measurements.

Samples. All the chemicals purchased from Tokyo Kasei were used as received. SDS aqueous micellar solutions (SDS solution) were prepared by stirring the sample solution for 3 days. The concentration of SDS was 0.1 M (M = mol dm^{-3}). Sample solutions were degassed by bubbling of Ar gas and were flowed through the cell. Sample cells are (1) a quartz flat cell with 0.3 mm interior space in TR-ESR measurements and (2) a quartz cell with light path lengths of 0.35 cm for excitation laser and 1.0 cm for monitor light in transient absorption measurements.

Results and Discussion

CIDEP of TEMPO in SDS Micelle. Figures 1a and 1b show TR-ESR spectra of TEMPO in SDS solutions obtained by 308 nm laser excitation of xanthone and bromopyrene, respectively. The gate was opened for 1.25–1.75 μs after the laser excitation. In these TR-ESR spectra, triplet peaks of TEMPO due to nitrogen atom appear with net microwave-emission (Em) CIDEP, which suggests that TEMPO radicals are spin polarized through photochemical processes. This CIDEP signal does not appear in the absence of xanthone or bromopyrene. This means that laser light excites xanthone (Fig. 1a) or bromopyrene (Fig. 1b) to the triplet state and CIDEP is generated by the interaction of TEMPO with these triplet molecules. Net Em CIDEP generation in the triplet-TEMPO system has been explained in terms of the quartet precursor (QP) RTPM as reported previously.[1,2,4,5] Similar spectra were observed in the systems of β-carotene, benzophenone, 1-chloronaphthalene and many other aromatic molecules–TEMPO in SDS solutions. These CIDEP can also be interpreted in terms of QP-RTPM in micelle.[5]

Although many systems in SDS solution gave net Em CIDEP of TEMPO due to QP-RTPM, some systems were found to show a different CIDEP pattern from the simple net Em type. Figure 1c and 1d show TR-ESR spectra obtained by 308 nm laser excitation of fluoranthene(Flt)– and pyrene(Py)–TEMPO in SDS solution, respectively. In these spectra, each hyperfine line of single net Em peak with Gaussian lineshape is deformed by overlapping of an antiphase EA (Em and enhanced microwave-absorption (Abs) in low and high field sides of single hyperfine line, respectively) polarization peak. The positions of APS in each spectrum coincide with those of hyperfine lines of TEMPO, suggesting that APS is attributed to a certain spin polarized TEMPO radical. In Figs. 1c and 1d, a single Abs peak is recognized between hyperfine lines of nuclear spin quantum number, $M_I = 0$ and -1. There are no other remarkably intense peaks except TEMPO, which suggests the possibility that the specie showing Abs peak does not have notable hyperfine structure. The g factor of this specie was determined as 1.9999 ± 0.0004. Murai and co-workers have reported that a spin polarized hydrated electron (e_{aq}^-) was detected in the system of xanthone in SDS solution by TR-ESR technique and the g factor of the e_{aq}^- was 2.00033 ± 0.00015.[12] The g factor of the Abs peak (1.9999 ± 0.0004) coincides with that of e_{aq}^- reported by Murai and co-workers, considering experimental error. Moreover, Py is known to yield Py cation (Py^+) radical and electron via a two-photon ionization process.[13] Therefore, we assigned these peaks to e_{aq}^-. To confirm our assignment, we observed TR-ESR spectrum of Py in SDS solution without TEMPO, as shown in Fig. 1e. A relatively sharp Abs peak is recognized whose resonance frequency coincides with that of the Abs peak assigned to e_{aq}^- in Fig. 1d. In this spectrum, a very broad band with weak net Em CIDEP appears in the lower field side of e_{aq}^-. We attributed this to Py^+ produced in the two-photon ionization of Py in SDS micelle. The linewidth of e_{aq}^- in the presence of TEMPO (Fig. 1d) seems much larger than that without TEMPO (Fig.

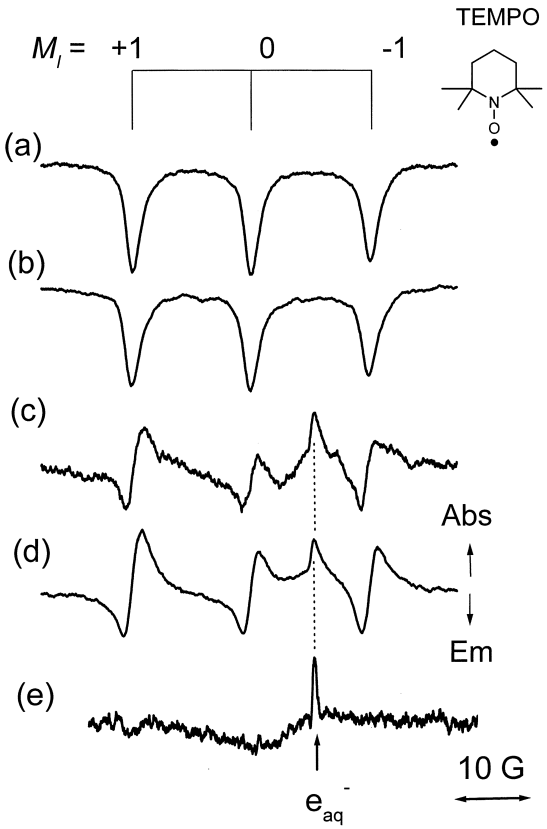

Fig. 1. TR-ESR spectra obtained by 308 nm laser excitation of SDS solution. Upper direction means signal with Abs and downward means Em signal. Sampling gate times after 308 nm laser excitation are 1.25–1.75 μs for (a) and (b), and 0.75–1.25 μs for others. Molecules dissolved in SDS solution were TEMPO (2 mM) with (a) xanthone (6.7 mM), (b) bromo-Py (0.4 mM), (c) Flt (4.6 mM), (d) Py (0.8 mM). (e) Py (0.8 mM) was dissolved in SDS solution without TEMPO.

1e). This may be attributed to the shorter spin relaxation time caused by TEMPO radical.

TR-ESR signals of e_{aq}^- in Py– and Flt–TEMPO systems are Abs. Both enhanced Abs CIDEP and Boltzman distribution of e_{aq}^- could be considered for this signal. In Fig. 1e, it is interesting that Py^+ shows almost net Em CIDEP, while e_{aq}^- indicates Abs signal. The typical g value of aromatic radical is ca. 2.002–2.003, which is larger than g value of e_{aq}^-. If these signals were created by a radical pair mechanism of geminate Py^+–e_{aq}^- pair, net Abs signal is reasonably explained by the large Δg value of ca. 0.002–0.003.[14] Unfortunately, we have no direct evidence to tell if the Abs signal is CIDEP.

The spectra shown above are not sufficient to determine the mechanism giving APS of TEMPO. In the following, we examine the Py–TEMPO system in much detail because excited state dynamics of Py has been extensively studied[13,15–18] and the intensity of APS signal in the Py–TEMPO system is very strong as seen in Fig. 1. The following intermediates may exist in the system under 308 nm laser excitation: the lowest excited singlet and triplet Py's (^{1}Py*, ^{3}Py*), Py^+ and e_{aq}^-. We examine the following three mechanisms as the origin of APS:

(1) Spin-Correlated Radical-Triplet Pair (SCRTP) of ^{3}Py* and TEMPO,

(2) SCRP of Py^+ and TEMPO,

(3) SCRP of e_{aq}^- and TEMPO.

According to mechanism (3), e_{aq}^- should show APS.[19] However, the e_{aq}^- in Fig. 1 shows a simple Abs line. Therefore, mechanism (3) is immediately excluded. Mechanism (2) is expected to give APS of TEMPO according to the SCRP theory. Concerning mechanism (1), there is no report on the spectrum of the SCRTP formed in the encounter process and it is not straightforward that APS is due to SCRTP. However, SCRTP with a small exchange interaction probably gives APS of TEMPO if one considers a similar mechanism with SCRP theory.

To distinguish the mechanisms (1) SCRTP of ^{3}Py*–TEMPO and (2) SCRP of Py^+–TEMPO, laser power dependence was measured for the CIDEP signal intensities. Figures 2a and 2b are the laser power dependences of APS signal at $M_I = +1$ peak of TEMPO and of the e_{aq}^- signal, respectively. The least square fitting of the plots gave the slopes of 1.77 for the APS signal and 1.96 for the e_{aq}^- signal. Both values are larger than 1 and close to 2, indicating that these signals require at least two photons. The ionization potential (*IP*) of Py in gas phase

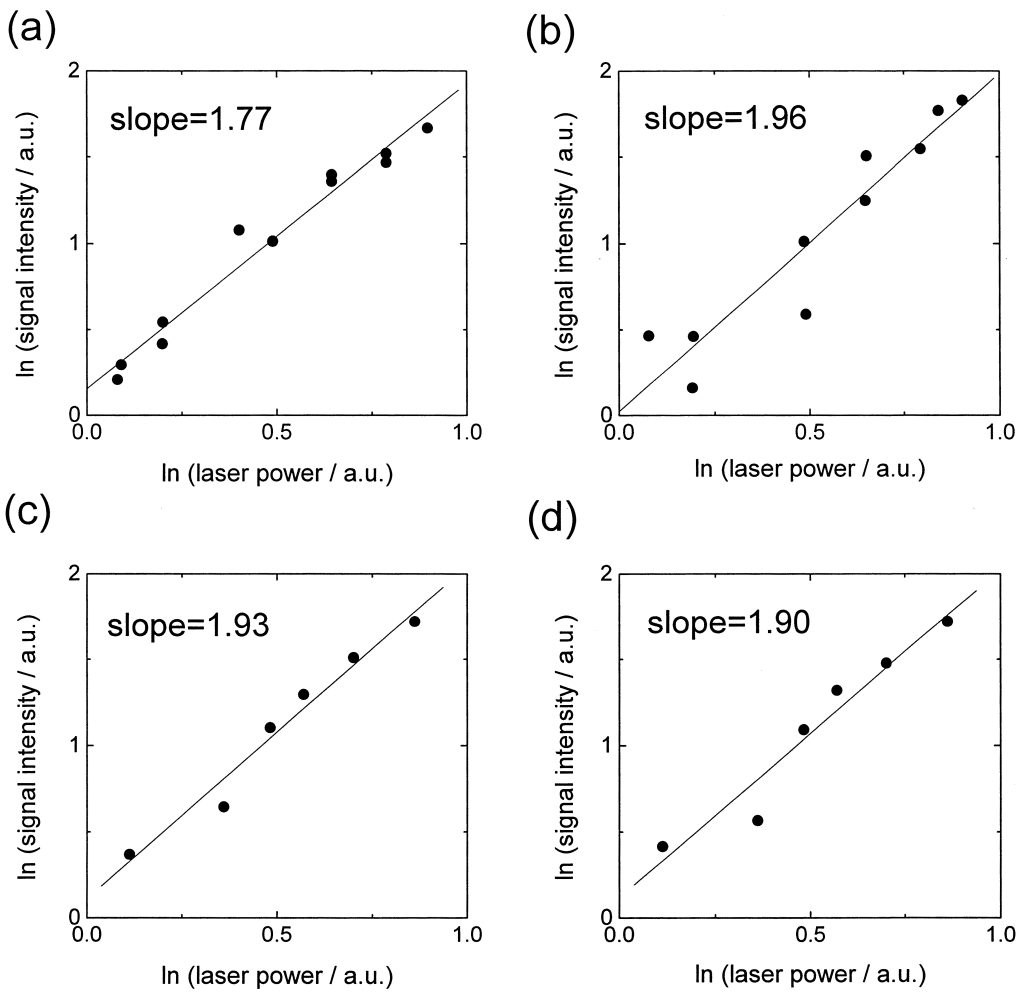

Fig. 2. Laser power dependence of CIDEP signals of TEMPO and e_{aq}^- in SDS solution. (a) and (b) are the signals in Py–TEMPO and, (c) and (d) are in Flt–TEMPO. Signal intensities were monitored at $M_I = +1$ peak of TEMPO for (a) and (c), and e_{aq}^- peak for (b) and (d).

is 7.41 eV and the S_1 energy of Py is 3.34 eV.[20] Since ionization threshold of a solute (I_s) is usually a few electron volts smaller than *IP* in gas phase, I_s of Py in SDS solution may be less than 7 eV. Wallace et al. estimated I_s of Py in condensed phase as 6.17 eV[13] by the equation considering polarization energy of Py^+ and the energy of excess electron state in liquid proposed by Raz and Jortner.[21] Therefore, two-photon absorption at 308 nm (4.03 eV) via the S_1 state brings about the photoionization of Py, which is consistent with the laser power dependence of the e_{aq}^- signal. APS signal also requires more than two photons, which means that a certain intermediate produced in two-photon process may yield the spin-correlated pair with TEMPO. Py^+, which is the counterpart of e_{aq}^- generated in photoionization process, is the product in biphotonic process; hence, APS signal can be explained by postulating SCRP of Py^+ and TEMPO generated in SDS micelle. On the other hand, $^3Py^*$ is generated through one-photon excitation and if APS is due to SCRTP of $^3Py^*$ and TEMPO, the APS signal must show linear power dependence. Therefore, we considered that mechanism (2) is responsible for the APS signal. The laser power dependence was also examined for the Flt–TEMPO system in SDS solution, as shown in Figures 2c and 2d. The e_{aq}^- and APS signals also show approximately square laser power dependence. *IP* of Flt in gas phase is 7.95 eV and the S_1 energy is 3.06 eV.[20] If we consider that I_s is usually lower than *IP* in gas phase, two-photon ionization via the S_1 state may be possible. Flt cation produced by the two-photon absorption is also related to the APS signal of TEMPO.

Though the existence of Py^+ was assumed in the SCRP mechanism in the above discussion, Py^+ was not clearly recognized in the TR-ESR spectra. The high viscosity of micelle interior causes the broadening of hyperfine structure of Py^+ with 10 protons, which may be responsible for the lack of a clear ESR signal of Py^+. To confirm the existence of Py^+ in the laser excitation of this system, transient absorption spectra were observed. Figure 3 shows the transient absorption spectra obtained by photoexcitation of Py in SDS solution without TEMPO at 1.0 μs after the laser pulse. Since the cell size used in the transient absorption experiment was different from that used in TR-ESR measurements, the optical density (OD) of Py at 308 nm was carefully controlled to be the same with that of TR-ESR experiment; OD was about 0.25 at 308 nm. There are two peaks at 415 and 450 nm which were assigned to the absorption of $^3Py^*$ and Py^+, respectively, according to the previous studies.[13,16] When the laser was not focused by a lens, the absorption at 415 nm is much stronger than that at 450 nm. On the other hand, when the laser was focused, the absorption at 450 nm is stronger than the absorption at 415 nm. This indicates that relative concentration of Py^+ to $^3Py^*$ becomes higher with increasing laser power. This result is consistent with the conclusion obtained above that Py^+ is produced by a biphotonic process while $^3Py^*$ is by one-photon process. Transient absorption decay of Py^+ without TEMPO monitored at 450 nm showed a very long lifetime of much more than 100 μs in SDS solution. Since most of the Py dissolved exists in micelle interior due to its hydrophobic property, Py^+ produced in micelle interior may be trapped by negative charges and thus, it is likely that Py^+ is lasting for more than 100 μs in micelle. Due to the relatively long lifetime of Py^+ in SDS micelle, Py^+ survives at the time window of TR-ESR measurement (a few microseconds after excitation) to yield APS of TEMPO.

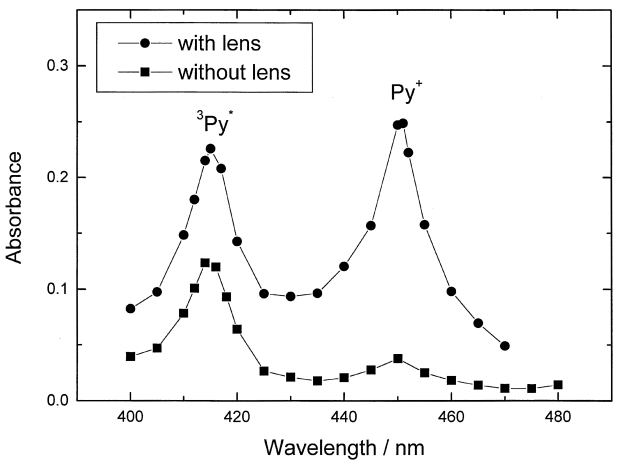

Fig. 3. Transient absorption spectra obtained by 308 nm laser excitation of Py (0.06 mM) in SDS solution system (without TEMPO). Signals were detected at 1.0 μs after laser excitation. The spectra were obtained with 308 nm laser focused with a lens or not.

To confirm Py^+–TEMPO SCRP mechanism for APS, we changed the relative concentration of $^3Py^*$ to Py^+ by adding quenchers and observed how TR-ESR spectrum altered. It has been reported that *p*-benzoquionone (BQ) is a good quencher for $^3Py^*$: BQ and $^3Py^*$ form a charge transfer complex, which is followed by the reaction yielding Py^+ and BQ anion.[16]

$$^3Py^* + BQ \rightarrow (Py^{\delta+} \cdots BQ^{\delta-}) \rightarrow Py^+ + BQ^- \qquad (1)$$

Figure 4a shows transient absorption spectra of Py in SDS solution with and without BQ. The transient absorption spectrum in the presence of BQ is very different from that without BQ: The strong band at 450 nm and a broad absorption around 430 nm of Py^+ appear but the sharp absorption band of $^3Py^*$ at 415 nm seen in the spectrum without BQ disappears in the presence of BQ. This result indicates that $^3Py^*$ is quenched by BQ and Py^+ is produced through reaction (1).

Figure 4b shows TR-ESR spectra in the system of Py–TEMPO with and without BQ. As seen from the spectrum, intensity of APS signal in the Py–TEMPO system with BQ is almost the same or slightly stronger than that in the Py–TEMPO system without BQ. One need not consider the contribution of photoexcited BQ because of its low optical density in these measurements. Though almost all of $^3Py^*$ was quenched in the presence of BQ, as seen in Fig. 4a, the signal intensity of APS was not affected. This is another piece of evidence for mechanism (2) but not for mechanism (1). A similar quenching experiment was carried out in the Py–TEMPO system with 1,4-cyclohexadiene as the $^3Py^*$ quencher and no decrease of APS signal intensity was recognized. These results definitely exclude mechanism (1) for APS and we conclude that APS is due to SCRP of Py^+ and TEMPO.

There are many reports on TR-ESR spectra of SCRP in micelle and in highly viscous solvents.[6–9] All of these SCRP is due to the geminate pair produced in the photoreaction pro-

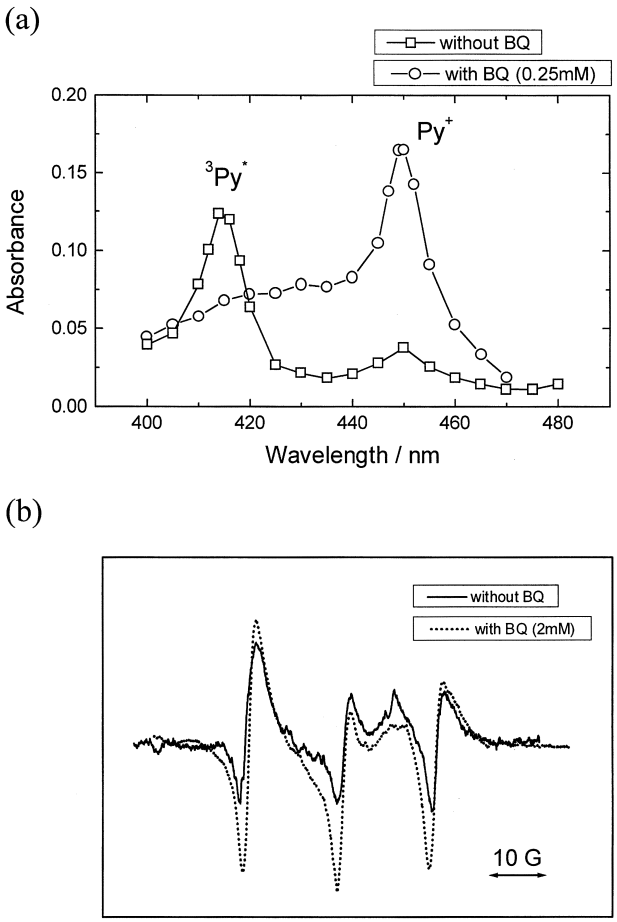

Fig. 4. (a) Transient absorption spectra of Py (0.06m M) in SDS solution system (without TEMPO) measured at 1.0 μs after laser pulse without BQ and in the presence of BQ (0.25 mM). (b) TR-ESR spectra of TEMPO in the Py (0.8 mM)–TEMPO (2 mM) system in SDS solution with or without BQ. The gate time was opened from 0.75 to 1.25 μs.

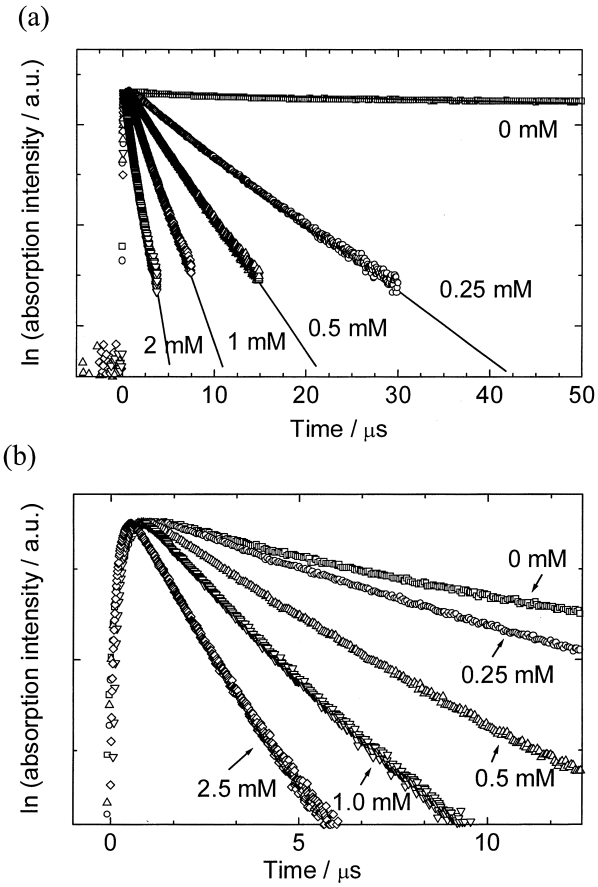

Fig. 5. Semi-logarithmic plots of transient absorption decays of (a) Py^+ and (b) $^3Py^*$ in SDS solution with various TEMPO concentrations. Decays were monitored at (a) 450 nm and (b) 415 nm, respectively. Absorption intensity in each decay are normalized at maximum value of absorbance in each decay.

cess. On the other hand, the present SCRP spectrum of Py^+ and TEMPO in SDS micelle is due to free encounter reaction. To the best of our knowledge, this is the first report on the SCRP spectrum of a free encounter reaction process.

Quenching Decay Rate Constants of Py^+ and $^3Py^*$ According to the results mentioned above, APS is due to SCRP of Py^+ and TEMPO while net Em is generated by RTPM of $^3Py^*$ and TEMPO. According to the theory of SCRP[7,8] and RTPM,[1,2] the reaction of Py^+ in SCRP and deactivation of $^3Py^*$ in RTPM are important for the generation of CIDEP. The following scheme is considered for the reaction of Py^+:

$$Py^+ + e^- \rightarrow Py$$

$$Py^+ + TEMPO \rightarrow {}^1(Py^+ \cdots TEMPO) \rightarrow {}^1Py + TEMPO^+ \text{ or other products} \quad \text{(reaction)}$$

$$\rightarrow {}^3(Py^+ \cdots TEMPO) \rightarrow Py^+ + TEMPO \quad \text{(collision)}$$

Encounter of Py^+ and TEMPO randomly forms both singlet and triplet pairs. The former selectively undergoes the reaction and the triplet SCRP of Py^+ and TEMPO survives in SDS micelle. Since APS observed in Fig. 1 shows Em in low and enhanced Abs in high field sides of each hyperfine line, the exchange interaction of Py^+ and TEMPO should be negative according to the SCRP theory.[7,8] On the other hand, CIDEP due to QP-RTPM of $^3Py^*$ and TEMPO is generated in the following deactivation process:

$$^2(^3Py^* \cdots TEMPO) \rightarrow {}^2(^1Py \cdots TEMPO) \rightarrow {}^1Py + TEMPO$$

Since $^3Py^*$ and Py^+ can be monitored by transient absorption measurements, an analysis of $^3Py^*$ and Py^+ decays versus TEMPO concentration was carried out to examine the reactivity of these species and eventually, to explain the time evolution of CIDEP in the Py–TEMPO system in SDS micelle.

Figure 5a shows the semi-logarithmic plots of the decay signal of Py^+ in SDS solution with various concentrations of TEMPO. All the plots are almost fitted to straight lines and the slope decreases with increase in the concentration of TEMPO. Since the decay component mainly reflects the time profile of Py^+ concentration in SDS micelle interior, this result suggests that Py^+ reacts with TEMPO in the micelle interior. Figure 5b show semi-logarithmic plots of $^3Py^*$ decays monitored at 415 nm. The transient absorption decays of $^3Py^*$ with and without TEMPO show single exponential decay functions. Fast rise at high concentration TEMPO seen in Fig. 5b is due to enhanced intersystem crossing by radical.

Most of Py and TEMPO do not dissolve in aqueous phase but in micelle interior. Therefore, ^{3}Py* is generated and reacts with TEMPO in SDS micelle interior. A micelle belongs to an inhomogeneous system and the kinetics is more complicated than that in conventional solvent. First of all, we estimate the concentration of SDS micelle according to the equation:[22,23]

$$[M] = ([SDS] - cmc)/N \quad (2)$$

where *cmc* is critical micelle concentration, N is average aggregation number of SDS micelle, and [M] is the concentration of SDS micelle. In the present experiments, [SDS] is 0.1 M in all cases. N and *cmc* of SDS micelle have been reported as 62 and 8.2 mM, respectively.[22] Substitution of these values in Eq. 2 yields [M] = 1.48×10^{-3} M which is larger than the concentration of Py (about 0.06 mM in transient absorption and about 0.8 mM in TR-ESR measurements). This means that the number of Py molecules dissolved in a unit micelle is less than one. On the other hand, the concentration of TEMPO is from 0 to 2.5 mM in the quenching experiment and thus, averaged occupation number of TEMPO in a micelle is less than 1 in some decay results. It is expected that the kinetics of Py in micelle with TEMPO differs from that without TEMPO and thus, some of the time profiles might show non exponential decay. However, most of the decays of Py^+ and ^{3}Py* with TEMPO concentration of 0–2.5 mM are characterized by a single exponential. Therefore, we assume that the intermicellar exchange of TEMPO and Py is important in the present system and the rapid fluctuation of TEMPO occupation number in a micelle gives exponential behavior in decay kinetics.[24] Under this assumption we analyzed the decay profiles by the equation:

$$k = k_0 + k_q[TEMPO] \quad (3)$$

An analysis of the transient absorption decay rates of ^{3}Py* and Py^+ versus the concentration of TEMPO is shown in Fig. 6.

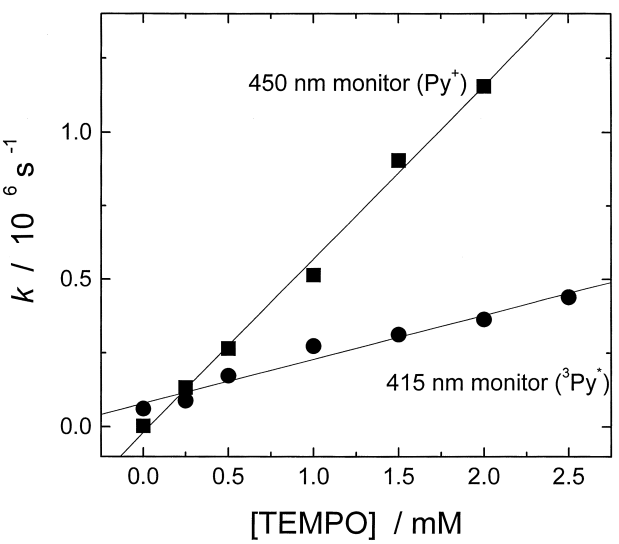

Fig. 6. Analysis of transient absorption decays of ^{3}Py* (circle) and Py^+ (rectangular) versus the concentration of TEMPO.

From the analysis of the slopes, the quenching rate constant of ^{3}Py* by TEMPO, $k_q(^3Py^*)$, and the reaction rate constant of Py^+ and TEMPO, $k_q(Py^+)$ were determined as $(1.5 \pm 0.12) \times 10^8$ and $(5.9 \pm 0.21) \times 10^8$ M^{-1} s^{-1}, respectively. It is noteworthy that $k_q(Py^+)$ is about four times as large as $k_q(^3Py^*)$.

The most probable reaction of Py^+ with TEMPO is electron transfer. The redox potentials, $E(Py^+/Py)$ and $E(TEMPO^+/TEMPO)$ have been reported as 1.17[20] and 0.68 V[25] in acetonitrille, respectively. We assume that the redox potentials in SDS micelle interior are almost the same as these in acetonitrile. According to these redox potentials, electron transfer between Py^+ and TEMPO is 0.49 V exothermic and thus, the reaction may be controlled by the diffusion process. On the other hand, ^{3}Py* quenching rate constant in acetonitrile is about a thousand times as small as the diffusion-controlled rate constant in acetonitrile.[26] This is because the energy of ^{3}Py* (16850 cm^{-1}) [20] is lower than D_1 energy of TEMPO (> 18000 cm^{-1})[2] and energy transfer is inaccessible. This suggests that the $k_q(^3Py^*)$ in SDS micelle interior may be smaller than the diffusion-controlled rate constant. Therefore, it is reasonable that $k_q(^3Py^*)$ is slower than $k_q(Py^+)$.

The reaction rates under the condition of TR-ESR measurement (TEMPO concentration = 2 mM) are estimated to be 3.0×10^5 s^{-1} for $k_q(^3Py^*)$ and 1.2×10^6 s^{-1} for $k_q(Py^+)$, respectively. Judging from these values, most of Py^+ may react with TEMPO through singlet channel to create CIDEP within the first a few μs after laser excitation. Therefore, the CIDEP with APS in the system of Py–TEMPO can be concluded to appear in our TR-ESR spectra through SCRP mechanism of Py^+ and TEMPO.

Simulation of TR-ESR Spectrum for Py^+–TEMPO SCRP. Figure 7 shows the TR-ESR spectra of Py–TEMPO system in SDS solution with various gate times. The CIDEP pattern of the spectrum with the gate time at 1.0 μs has already been interpreted in terms of SCRP of Py^+–TEMPO as discussed above. The TR-ESR spectra with the gates at 3.5 and 4.0 μs are dominated by net Em type CIDEP, which may be interpreted in terms of RTPM of ^{3}Py*–TEMPO. In the time region of 0.75–3.0 μs, TR-ESR spectra consist of APS signal due to SCRP and net Em polarization due to RTPM. In a qualitative way, we understood this time evolution of SCRP and RTPM signals on the basis of $k_q(Py^+)$ and $k_q(^3Py^*)$ values together with spin-lattice relaxation time. Since the concentration of SDS micelle (1.48 mM) is smaller than that of TEMPO (2 mM), the averaged occupation number of TEMPO in a micelle is ca. 1.35 and thus, both SCRP and RTPM signal rise times may depend on encounter rates of TEMPO with Py^+ and ^{3}Py*, respectively, within the micelle. Encounter rates correspond to the diffusion rate in the micelle and are almost identical. On the other hand, decay rates of SCRP and RTPM are controlled by $k_q(Py^+)$ and $k_q(^3Py^*)$, respectively, together with the corresponding spin-lattice relaxation times. Spin-lattice relaxation time of TEMPO in paraffin oil at room temperature is reported as 0.51 μs[27] which is much shorter than deactivation time of ^{3}Py* (3.3 μs) and thus, decay rate of RTPM may be close to the deactivation rate. This decay rate of RTPM is obviously slower than the reaction time of Py^+ (0.83 μs), which is the upper limit value of SCRP signal decay time. Therefore, the decay time of RTPM signal is probably longer

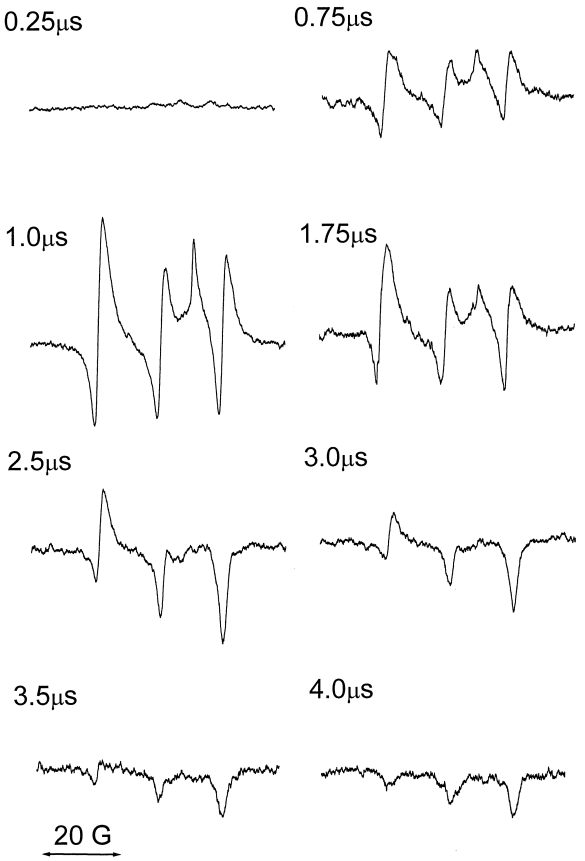

Fig. 7. Time evolution of TR-ESR spectra of TEMPO measured at 308 nm laser excitation of Py (0.8 mM)–TEMPO (2 mM) system in SDS (0.1 M) solution.

than that of SCRP signal. The time evolution of TR-ESR spectrum should reflect the sum of mutually independent time evolution of CIDEP's in Py^+- and $^3Py^*$–TEMPO systems and thus, the SCRP signal appears only in the spectra at early gate times, while the relative intensity ratio of net Em due to QP-RTPM becomes dominant in the spectra with late gate times. In order to confirm these assignments of CIDEP and its time profile, we performed a simple simulation of CIDEP pattern. In the simulation, the intensity ratio of CIDEP mechanisms, SCRP and RTPM, was assumed to depend on the gate time. For the simulation of SCRP, the theory proposed by Mclauchlan and his co-workers was adopted.[7] At the beginning, spin-lattice relaxation was not considered. When two radicals are fixed at a separation r where the exchange interaction is $J(r)$, the spin Hamiltonian, $H(r)$ of the radical pair is written by:

$$H(r) = \beta(g_a S_a + g_b S_b)H_0 + \sum_n A_{an} I_{an} S_a + \sum_m A_{bm} I_{bm} S_b - J(r)\{2S_a S_b + \frac{1}{2}\}$$

where, β, g_a, g_b, S_a, S_b, H_0, A_{an}, A_{bm}, I_{an} and I_{bm} have their usual meanings.[7] Then the eigenstates, $|i\rangle$, and eigenvalues, ω_i of the Hamiltonian are

$|1\rangle = |T_{+1}\rangle$ $\omega_1 = -J + \omega$,
$|2\rangle = \cos\psi|S\rangle + \sin\psi|T_0\rangle$ $\omega_2 = \Omega$,
$|3\rangle = \mathrm{vsin}\,\psi|S\rangle + \cos\psi|T_0\rangle$ $\omega_3 = -\Omega$,
$|4\rangle = |T_{-1}\rangle$ $\omega_4 = -J - \omega$.

where

$\omega = (\omega_A + \omega_B)/2$, $Q = (\omega_A - \omega_B)/2$,
$\Omega^2 = J^2 + Q^2$, $\tan 2\psi = Q/J$

In the present system, a free encounter pair of Py^+ and TEMPO is considered and thus we assume the triplet radical pair. The population $P(|i\rangle)$ of state i under this condition is 1/3 for $i = 1, 4$, and are $1/3\sin^2\psi$ and $1/3\cos^2\psi$ for $i = 2$ and 3, respectively. The intensity of ESR transition, I_{ij} is thus obtained as shown below:

$$-I_{12} = -I_{13} = I_{24} = I_{34} = \frac{1}{12}\sin^2 2\psi = \frac{Q^2}{12\Omega^2}.$$

In the presence of spin relaxation such as J fluctuation, population ratio of $|2\rangle$ and $|3\rangle$ changes and hence the intensities of four possible ESR transitions are no longer equivalent.[28] We express the extent of this spin relaxation $\Delta P(|2\rangle)$ by $x(\%)$, which follows the equation

$$\Delta P(|2\rangle) = \frac{|P(|2\rangle) - P'(|2\rangle)|}{2} \times \frac{x(\%)}{100}.$$

where $P(|2\rangle)$ and $P'(|2\rangle)$ mean populations of state $|2\rangle$ before and after the spin relaxation from $|2\rangle$ to $|3\rangle$, respectively.

By using this theory for SCRP, we performed the simulation of TR-ESR spectra. The following values were used in the simulation: g(TEMPO): 2.00583, A_N: 16.86 G (both from experiments), A_H of hydrogen atoms in Py^+: 5.4 G for 4H, 1.2 G for 2H, and 2.1 G for 4H,[29] $J(r)$: 0.3 G (estimated from the splitting of the peaks), linewidth: 1.8 G for each APS. There is no report on g value of (Py^+) as far as we know, so we adopted the value 2.002569, which is the g value of perylene cation.

Figure 8a is the simulated ESR spectra of TEMPO considering only the net emission due to RTPM. Figures 8b, 8c and 8d show the simulated spectra for the SCRP. The $x(\%)$ values used in these spectra are 0, 50, and 100%. As seen in these spectra, the intensity pattern of APS depends strongly on the spin relaxation. Since the present TR-ESR spectrum is the blend of CIDEP's due to SCRP and RTPM, TR-ESR spectra at various gate times were reproduced by the sum of the simulated spectra of RTPM (Fig. 8a) and SCRP (Figs. 8b, 8c, or 8d). Figure 9 shows TR-ESR spectra of Py–TEMPO in SDS solution together with the simulated spectra. The extent of spin relaxation of SCRP and the intensity ratio of RTPM and SCRP were determined for each spectrum from the best fitted simulation. Since we did not consider the CIDEP of e_{aq}^- in the model for simulation, the sharp Abs peak is not superimposed on the simulation spectra. Py^+ has many hyperfine lines and the peaks of Py^+ with APS become very broad. This may be why Py^+ signal is hardly recognized in the TR-ESR spectra. The fitting of the spectra seems suitable at the gate times of 0.75, 1.0 and 1.75 μs, but rather bad at 2.5 and especially, at 4.0 μs. As clearly seen in the observed spectrum at 4.0 μs, emission intensity at $M_I = +1$ peak is much weaker than that at $M_I = -1$ peak. Addition of A/E (enhanced Abs in low field side and Em in high field side) type CIDEP of TEMPO to the simulated spectrum at 4.0 μs may improve the fitting. One of the candidates of A/E-type CIDEP mechanism is the radical pair mechanism[3] in the reaction of e_{aq}^- and TEMPO with positive J

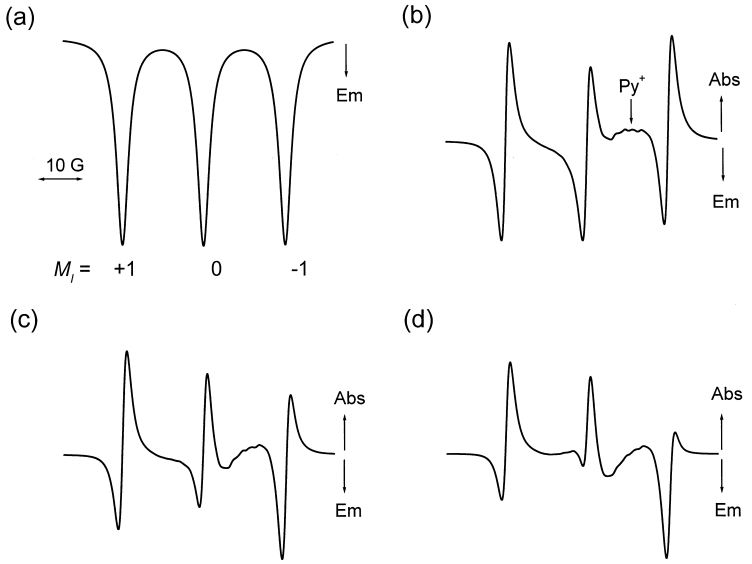

Fig. 8. The simulated spectra of TEMPO for (a) RTPM, (b) SCRP mechanism without spin relaxation between the states $|2\rangle$ and $|3\rangle$, (c) 50% spin relaxation, and (d) 100% spin relaxation. The parameters used in the simulation were, g(TEMPO) = 2.00583, $g(Py^+)$ = 2.002569, $J = -0.3$ G, and line width = 1.2 G (RTPM) or 1.8 G (APS).

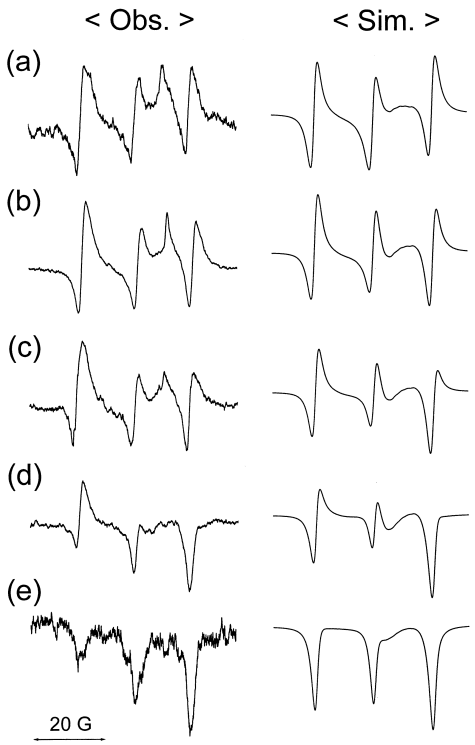

Fig. 9. TR-ESR spectra of TEMPO in Py–TEMPO system measured at (a) 0.75, (b) 1.0, (c) 1.75, (d) 2.5, and (e) 4.0 μs after laser excitation with 0.5 μs gate width together with the simulated spectra. The CIDEP mechanisms in each simulated spectrum were (a) SCRP without spin relaxation, (b) SCRP with 30% spin relaxation, (c) SCRP with 50% spin relaxation and RTPM, and (d) and (e) SCRP with 100% spin relaxation and RTPM. Intensity ratio of SCRP to RTPM were (c) 10:3, (d) 5:4 and (e) 3:10. The spectra of SCRP or RTPM are normalized at the most intense line of each SCRP and RTPM spectrum.

value. Since the A/E CIDEP seems to rise with e_{aq}^- signal decaying around 1.75 μs, the reaction of e_{aq}^- with TEMPO could be responsible for A/E CIDEP after 2.0 μs.

The simulation of TR-ESR spectra at various gate times leads us to conclude that there are at least two CIDEP mechanisms, SCRP of Py^+–TEMPO and RTPM of $^3Py^*$–TEMPO in Py–TEMPO dissolved in SDS solution, and that the time evolution of CIDEP from APS-type to net Em-type is interpreted as the mutually independent time evolutions of CIDEP in TEMPO with SCRP and RTPM.

RTPM creates CIDEP in SDS micelle, which indicates that there are triplet-TEMPO pairs in SDS micelle. However, we concluded that there is no signal of SCRTP between TEMPO and triplet molecule in the present TR-ESR spectra. This may be understood if we assume these triplet-TEMPO pairs do not create strong CIDEP. The spin-lattice relaxation time of triplet molecule is usually several ten nanoseconds or less in the fluid solution at the room temperature. If a very fast spin-lattice relaxation averages out the population difference in the radical-triplet sublevels, transition intensities between the sublevels decrease to be zero and no polarized spectra should be observed in any triplet-TEMPO systems. To observe TR-ESR spectra of radical-triplet encounter pairs at room temperature, it may be important to increase spin-lattice relaxation somehow.

References

1 C. Blättler, F. Jent, and H. Paul, *Chem. Phys. Lett.*, **166**, 375 (1990).

2 A. Kawai, T. Okutsu, and K. Obi, *J. Phys. Chem.*, **95**, 9130 (1991); A. Kawai and K. Obi, *Res. Chem. Intermed.*, **19**, 866 (1993).

3 For example, A. Carrington and A. D. McLachlan, "Introduction to Magnetic Resonance with Application to Chemistry and Chemical Physics," Harper and Row, New York (1967); L.

Devan and M. K. Bowman, "Mordern Pulsed and Continuous-Wave Electron Spin Resonance," John Wiley and Sons (1990); L. T. Muss, P. W. Atkins, K. A. McLauchlan and J. B. Pedersen, "Chemically Induced Magnetic Polarization," Reidel, Dordrecht (1977); Y. N. Molin, "Spin Polarization and Magnetic Effects in Radical Reactions" Wiley-Interscience, New York (1973).

4 A. Kawai and K. Obi, *J. Phys. Chem.*, **96**, 52 (1992); Y. Kobori, A. Kawai, and K. Obi, *J. Phys. Chem.*, **98**, 6425 (1994); Y. Kobori, M. Mitsui, A. Kawai, and K. Obi, *Chem. Phys. Lett.*, **252**, 355 (1996); M. Mitsui, K. Takada, Y. Kobori, A. Kawai, and K. Obi, *Chem. Phys. Lett.*, **262**, 125 (1996); A. Kawai, M. Mitsui, Y. Kobori, and K. Obi, *Appl. Magn. Reson.*, **12**, 405 (1997); A. Kawai, K. Shibuya, and K. Obi, *Appl. Magn. Reson.*, **18**, 343 (2000).

5 A. Kawai and K. Obi, *J. Phys. Chem.*, **96**, 5701 (1992).

6 H. Murai, Y. Sakaguchi, H. Hayashi, and Y. J. I'Haya, *J. Phys. Chem.*, **90**, 113 (1986).

7 C. D. Buckley, D. A. Hunter, P. J. Hore, and K. A. McLauchlan, *Chem. Phys. Lett.*, **133**, 307 (1987).

8 G. L. Closs, M. D. E. Forbes, and J. R. Norris, Jr., *J. Phys. Chem.*, **91**, 3592 (1987).

9 K. Tominaga, S. Yamauchi, and N. Hirota, *J. Chem. Phys.*, **92**, 5175 (1990).

10 H. Murai, T. Imamura, and K. Obi, *Chem. Phys. Lett.*, **97**, 295 (1982).

11 Y. Kajii, M. Fujita, H. Hiratsuka, K. Obi, Y. Mori, and I. Tanaka, *J. Phys. Chem.*, **91**, 2791 (1987).

12 N. Ishiwata, H. Murai, and K. Kuwata, *J. Phys. Chem.*, **97**, 7129 (1993).

13 S. C. Wallace, M. Grätzel, and J. K. Thomas, *Chem. Phys. Lett.*, **23**, 359 (1973), and references therein.

14 H. Murai, and K. Kuwata, Chem. Phys. Lett., 164, 567 (1989); A. S. Jeevarajan and R. W. Fessenden, J. Phys. Chem., 96, 1520 (1992).

15 P. L. Piciulo, and J. K. Thomas, *J. Chem. Phys.*, **68**, 3260 (1978).

16 A. Kira, S. Arai, and M. Imamura, *J. Chem. Phys.*, **54**, 4890 (1971).

17 F. Wilkinson, J. Shroeder, *J. Chem. Soc. Faraday. Trans. 2*, **75**(3), 441 (1979).

18 S. N. Batchelor, H. Heikkilä, C. W. M. Kay, K. A. McLauchlan, and I. A. Shkrob, *Chem. Phys.*, **162**, 29 (1992).

19 K. Nakagawa, A. Katsuki, S. Tero-Kubota, N. Tsuchihashi, and T. Fujita, *J. Am. Chem. Soc.*, **118**, 5782 (1996).

20 S. L. Murov, I. Carmichael, and G. L. Hug, "Handbook of Photochemistry," Marcel Dekker, Inc. (1993).

21 B. Raz, and J. Jortner, *Chem. Phys. Lett.*, **4**, 155 (1969).

22 M. A. J. Rodgers and M. F. Da Silva E Wheeler, *Chem. Phys. Lett.*, **53**, 165 (1978).

23 N. J. Turro and A. Yekta, *J. Am. Chem. Soc.*, **100**, 5951 (1978).

24 M. A. J. Rodgers and M. F. Da Silva E Wheeler, *Chem. Phys. Lett.*, **42**, 587 (1976).

25 A. Samanta, K. Bhattacharyya, P. K. Das, P. V. Kamat, D. Weir, and G. L. Hug, *J. Phys. Chem.*, **93**, 3651 (1989).

26 J. C. Scaiano, "Handbook of Organic Photochemistry," CRC Press, Inc. (1989).

27 C. P. Poole, Jr, and H. A. Farach, "Handbook of Electron Spin Resonance," AIP Press, (1994).

28 M. Terazima, K. Maeda, T. Azumi, Y. Tanimoto, N. Okada, and M. Itoh, *Chem. Phys. Lett.*, **164**, 562 (1989); T. Fukuju, H. Yashiro, K. Maeda, H. Murai, and T. Azumi, *J. Phys. Chem. A*, **101**, 7783 (1997).

29 A. C. Buchanan III, R. Rivingston, A. S. Dworkin, and G. P. Smith, *J. Phys. Chem.*, **84**, 423 (1980).